Approximate Closed-Loop Minimax Model Predictive Operation Control of Microgrids

Christian A. Hans, Vladislav Nenchev, Jörg Raisch and Carsten Reincke-Collon

Abstract— We address an optimal control problem for a microgrid in islanded operation with bounded uncertain load and renewable infeed. While model predictive control (MPC) with worst-case cost evaluation is often employed to obtain robust optimal control laws in the presence of bounded disturbances, it suffers from an inherent conservativeness. To counteract this phenomenon, we propose an approximate closed-loop minimax MPC scheme, where the renewable energy sources output can be curtailed. The MPC is formulated as a mixed-integer linear program, solved online and applied in a receding horizon fashion. In the case study, the approximate closed-loop approach yields a better prediction accuracy and performance than the corresponding open-loop scheme.

I. INTRODUCTION

Active distribution networks provide an energy supply solution that is expected to cope with the increasing energy demand in a sustainable manner [1]. A particular type thereof are microgrids (MGs), i.e. small energy systems comprising thermal and renewable generation, storage units and loads connected over a (small) regional network. MGs can be operated in a grid-connected or in an islanded mode. This increases the reliability of the local grid, in the case when errors occur in the transmission network [2]. Also, due to infrastructural or geographical factors, some MGs are always operated in islanded mode. However, in this operation storage and consumption have to be balanced locally.

Optimising the operation of MGs with respect to available forecasts, while taking into account possible disturbances, is a challenging task. Recently, numerous MPC-based approaches have been proposed for related problems. Many schemes assume the presence of a perfect forecast, such as [3], e.g. based on the energy hub framework of [4], which also incorporates storage dynamics. This model has also been used in [5] to optimise operation in a risk-based manner. In [6] the economically optimal operation of MGs, based on an alternative model that specifically allows turning the units on and off, was emphasised. A hybrid method for minimising the costs for energy consumption for individual households with renewable energy sources (RES) while taking into account the expected energy demand, prices, and operational constraints was proposed in [7]. Many robust optimisation

approaches were also employed to tackle the closely related unit commitment problem. In [8], stochastic disturbances were taken into account in a reliability constrained problem and solved by an adaptive strategy. Uncertain forecasts of load and RES infeed were considered in a unified stochastic and robust approach [9]. A comparison of the performance of minimax and stochastic optimisation was provided in [10]. However, in most unit commitment approaches, the dynamics of storage units are neglected.

Due to high initial investments and low running costs of RES, it is naturally desired to maximise their infeed, which leads to a decreased fuel consumption by thermal generators. The latter should only be used when stored and current RES power cannot match the load. In times of high radiation and/or wind speed the power surplus can be used to charge storage units. RES infeed can be curtailed by adapting the power set points of the units if storage facilities are completely charged or a power limit is reached. This possibility was exploited in [11] to propose a robust MPC that takes into account the dynamics of storage devices and bounded forecast uncertainties for the load and RES. The motivation for using MPC was the high impact of the uncertain storage state on the optimal control trajectories. The approach was based on an open-loop minimax (OLMM) policy to obtain an input trajectory that minimises the worst-case performance, which, in general, leads to a conservative solution.

Leveraging ideas from [12], [13] and [14], our contribution extends the OLMM scheme of [11] by taking into account the dependence of predicted controls on the state forecasts in the optimisation procedure. We do this by using approximate closed-loop minimax (ACLMM) MPC, in which a parametrisation of the future inputs on the predicted disturbance is employed, yielding a better prediction accuracy and lower costs than the OLMM scheme.

The outline of the paper reads as follows. In Section II, we introduce notation and summarise some aspects from graph theory and DC power flow. Then, some assumptions, the model and its constraints leading to the problem formulation are presented. In Section III the ACLMM approach is described. In a numerical case study in Section IV, we compare the ACLMM with an OLMM and a mean certainty-equivalence approach.

II. PROBLEM FORMULATION

In this section, the optimal control problem (OCP) that formalises the task of reducing thermal power and increasing RES infeed in the presence of uncertainties is described. We start by introducing some notation.

C. A. Hans and V. Nenchev are with Technische Universität Berlin, Germany, {hans,nenchev}@control.tu-berlin.de

J. Raisch is with Technische Universität Berlin and Max-Planck-Institut für Dynamik komplexer technischer Systeme, Germany, raisch@control.tu-berlin.de

C. Reincke-Collon is with Younicos AG, Germany, reincke-collon@younicos.com

A. Preliminaries

We define the sets $\mathbb{R}_+ = \{x \in \mathbb{R} | x > 0\}$ and $\mathbb{R}_{0+} = \{x \in \mathbb{R} | x \geq 0\}$. Boolean variables are elements of the set $\mathbb{B} = \{0, 1\}$. The cardinality of a set $\mathcal{V}$ is denoted by $|\mathcal{V}|$. Let $\text{diag}(a_1, \ldots, a_n)$ denote the $n \times n$ diagonal matrix with diagonal entries a_i, $i = 1, \ldots, n$ and $\mathbf{I}_n$ the $n \times n$ identity matrix. Further, $\mathbf{0}_{nm}$ is the $n \times m$ matrix of all zeros and $\mathbf{1}_{nm}$ the matrix of all ones. Consequently, $\mathbf{0}_{n1}$ is the $n \times 1$ zero vector and $\mathbf{1}_{n1}$ the $n \times 1$ vector of ones. The element-wise absolute value of a vector V is denoted by $|V|$.

A *network is modelled* as a weighted, undirected, connected graph, i.e. a triple $\mathcal{G} = (\mathcal{V}, \mathcal{E}, \mathcal{W})$, where $\mathcal{V} = \{1, \ldots, v\}$ is the set of nodes and $\mathcal{E} = \{\bar{e}_1, \ldots, \bar{e}_e\}$, the set of undirected edges with $|\mathcal{E}| = e$. The $\tilde{e}$-th edge connecting node i and j is denoted as $\bar{e}_{\tilde{e}} \in \mathcal{E}$. The weight of every edge is given by the function $\mathcal{W} : \mathcal{E} \rightarrow \mathbb{R}_+$. The set of nodes is partitioned into five subsets $\mathcal{V}_\mathcal{D}$, $\mathcal{V}_\mathcal{R}$, $\mathcal{V}_\mathcal{S}$, $\mathcal{V}_\mathcal{T}$ and $\mathcal{V}_\mathcal{N}$. Elements of $\mathcal{V}_\mathcal{D}$ represent connected loads, elements of $\mathcal{V}_\mathcal{R}$ RES, elements of $\mathcal{V}_\mathcal{S}$ storage units, elements of $\mathcal{V}_\mathcal{T}$ thermal generators and elements of $\mathcal{V}_\mathcal{N}$ passive nodes, i.e. the nodes where no equipment is connected. In this framework, the utility grid is represented by a thermal generator with high nominal power as part of $\mathcal{V}_\mathcal{T}$ and the RES nodes in $\mathcal{V}_\mathcal{R}$ are only controllable in the sense that their power output can be limited. Let $|\mathcal{V}_\mathcal{D}| = d$, $|\mathcal{V}_\mathcal{R}| = r$, $|\mathcal{V}_\mathcal{S}| = s$, $|\mathcal{V}_\mathcal{T}| = t$ and $|\mathcal{V}_\mathcal{N}| = n$. The number of all (partly) controllable nodes is denoted by $h = t + s + r$, and the number of uncertain variables by $m = d + r$. Power lines are represented by the edges $\bar{e}_{\tilde{e}}$ connecting different nodes. By choosing for every edge $\bar{e}_{\tilde{e}} \in \mathcal{E}$ an arbitrary direction, the node-edge incidence matrix $\mathcal{F} \in \mathbb{R}^{v \times e}$ is defined element-wise as

$$\mathcal{F}_{i\tilde{e}} = \begin{cases} 1 & \text{if node } i \text{ is the sink of edge } \bar{e}_{\tilde{e}} \\ -1 & \text{if node } i \text{ is the source of edge } \bar{e}_{\tilde{e}} \\ 0 & \text{else.} \end{cases}$$

Power flow in an AC network is connected with the power of the nodes in a nonlinear way [15]. In order to obtain a linear relation between these quantities, we assume that voltage differences (in angle and amplitude) are small and line resistances are negligible (lossless lines). Hence, the linearised DC power flow equations can be used [16]. Then, the power flow $P_\mathcal{E} \in \mathbb{R}^e$ over the (inductive) lines is calculated with the phase angles of the nodes $\Theta \in \mathbb{R}^v$ by $P_\mathcal{E} = \text{diag}(y_1, \ldots, y_e) \mathcal{F}^T \Theta$, where $y_{\tilde{e}} = \mathcal{W}(\bar{e}_{\tilde{e}})$ for $\tilde{e} \in [1, e] \subset \mathbb{N}$ are the edge weights. The connection between $\Theta = (\theta_1, \ldots, \theta_v)^T$ and the power injected by the nodes $P_\mathcal{V} = (p_1, \ldots, p_v)^T$ is given by the DC power flow model

$$P_\mathcal{V} = \mathbf{Y}\Theta, \tag{1}$$

where $\mathbf{Y} = \mathcal{F} \text{diag}(y_1, \ldots, y_e) \mathcal{F}^T$, $\mathbf{Y} \in \mathbb{R}^{v \times v}$ is the Laplacian matrix. As $\mathcal{G}$ is undirected and connected, $\mathbf{Y}$ is symmetric and has rank $v - 1$. Therefore, we introduce

$$\begin{pmatrix} \tilde{\Theta} \\ \theta_v \end{pmatrix} = \underbrace{\begin{pmatrix} \mathbf{I}_{v-1} & -\mathbf{1}_{(v-1)1} \\ \mathbf{0}_{1(v-1)} & 1 \end{pmatrix}}_{\mathbf{T}} \Theta = \begin{pmatrix} \theta_1 - \theta_v \\ \vdots \\ \theta_v \end{pmatrix}. \tag{2}$$

Inserting (2) into (1) with $P_\mathcal{V} = (\tilde{P}_\mathcal{V}^T, p_v)^T$ leads to

$$\begin{pmatrix} \tilde{P}_\mathcal{V} \\ p_v \end{pmatrix} = \mathbf{Y}\mathbf{T}^{-1}\begin{pmatrix} \tilde{\Theta} \\ \theta_v \end{pmatrix} = \begin{pmatrix} \tilde{\mathbf{Y}} & \mathbf{0}_{(v-1)1} \\ b^T & 0 \end{pmatrix}\begin{pmatrix} \tilde{\Theta} \\ \theta_v \end{pmatrix}, \tag{3}$$

where with $\tilde{\mathbf{T}} = (\mathbf{I}_{v-1}, \mathbf{0}_{(v-1)1})$, $\tilde{\mathbf{Y}} = \tilde{\mathbf{T}}\mathbf{Y}\tilde{\mathbf{T}}^T$ is non-singular (see [17]), and $b^T = (\mathbf{0}_{1(v-1)}, 1)\mathbf{Y}\tilde{\mathbf{T}}^T$. Inserting $\tilde{\mathbf{Y}}$, we get

$$P_\mathcal{E} = \text{diag}(y_1, \ldots, y_e) \mathcal{F}^T \mathbf{T}^{-1}\begin{pmatrix} \tilde{\mathbf{Y}}^{-1}\tilde{P}_\mathcal{V} \\ \theta_v \end{pmatrix}. \tag{4a}$$

Note that the last row of (3), given by

$$p_v = b^T \tilde{\mathbf{Y}}^{-1} \tilde{P}_\mathcal{V}, \tag{4b}$$

ensures that the sum of all generated and consumed power equals zero. For $\theta_v = 0$, (4) can be rewritten with the constants $\mathcal{F}' = \text{diag}(y_1, \ldots, y_e) \mathcal{F}^T \mathbf{T}^{-1}\tilde{\mathbf{T}}^T \tilde{\mathbf{Y}}^{-1}\tilde{\mathbf{T}}$, $\mathcal{F}' \in \mathbb{R}^{e \times v}$ and $b' = (b^T \tilde{\mathbf{Y}}^{-1}, -1) \in \mathbb{R}^{1 \times v}$ as

$$P_\mathcal{E} = \mathcal{F}' P_\mathcal{V}, \tag{5a}$$

$$0 = b' P_\mathcal{V}. \tag{5b}$$

B. Assumptions

In the following, we assume that *i)* as explained in the previous paragraph, the voltage amplitude is constant, the voltage angle differences small and the line resistance is neglected (i.e. we can use the DC power flow equations); the error introduced by this simplification is small compared to the uncertainty that comes from the load and the RES; *ii)* the storage devices and the thermal generators can form the grid and run as voltage sources providing frequency and voltage; if they run in parallel they share the variations in power coming from the RES and the load through a decentralised droop-control mechanism, similar to [18]; because the dynamics of this mechanism evolve on a much faster time-scale, this power sharing is assumed to be instantaneous; *iii)* the time constants of the non negligible part of the storage dynamics are in the range of several minutes; hence, it is sufficient to solve the OCP on the same time scale; *iv)* no communication failures between the MPC and the units occur; also the communication delay is assumed to be negligible compared to the sampling time of the MPC; *v)* the error caused by the conversion losses and the self-discharge of the storage device are negligible compared to the disturbance caused by the load and the RES; if needed, this assumption could be easily dropped as show in [6]; *vi)* reactive power can be neglected (for simplicity); hence, the line limits are only approximately accounted for; *vii)* forecasts for the load and RES infeed are available in form of time varying lower and upper bounds.

C. Modelling and Constraints

We work in a discrete time framework with sampling interval $t_S \in \mathbb{R}_+$, typically in the domain of minutes. The state vector $x_k = E_{\mathcal{S},k}$ represents the stored energy in every node of $\mathcal{V}_\mathcal{S}$ at time kt_S, $k \in \mathbb{N}_0$. Further, u_k, δ_k and w_k refer to a real valued input, a Boolean input and a disturbance at time kt_S. The vector $u_k = (u_{\mathcal{T},k}^T, u_{\mathcal{S},k}^T, u_{\mathcal{R},k}^T)^T$ represents the power set points of the thermal generation units $u_{\mathcal{T},k} \in \mathbb{R}_{0+}^t$, the storage devices $u_{\mathcal{S},k} \in \mathbb{R}^s$ and the RES $u_{\mathcal{R},k} \in \mathbb{R}_{0+}^r$.

The Boolean input $\delta_k = (\delta_{\mathcal{T},k}^T, \delta_{\mathcal{S},k}^T, \delta_{\mathcal{R},k}^T)^T$ indicates which units are running, where $\delta_{\mathcal{T},k} \in \mathbb{B}^t$ refers to the thermal generators. $\delta_{\mathcal{S},k} \in \mathbb{B}^s$ and $\delta_{\mathcal{R},k} \in \mathbb{B}^r$ indicate which storage unit or RES is running. Disturbances $w_k = (w_{\mathcal{D},k}^T, w_{\mathcal{R},k}^T)^T$ represent the variation of the load demand, $w_{\mathcal{D},k} \in \mathbb{R}^d$, and variations due to fluctuation of the RES, $w_{\mathcal{R},k} \in \mathbb{R}^r$. Note that δ_k and u_k are control variables that satisfy the implication $(\delta_k)_{\tilde{h}} = 0 \Rightarrow (u_k)_{\tilde{h}} = 0 \ \forall \tilde{h} \in [1, h] \subset \mathbb{N}$, i.e. the power of a disabled unit is zero.

For convenience, we introduce the vectors $X_k = (x_{k|k}^T, \ldots, x_{k+K-1|k}^T)^T$ denoting the predicted values of the state, $U_k = (u_{k|k}^T, \ldots, u_{k+K-1|k}^T)^T$ denoting the real-valued inputs, $\Delta_k = (\delta_{k|k}^T, \ldots, \delta_{k+K-1|k}^T)^T$ denoting the Boolean inputs, and $W_k = (w_{k|k}^T, \ldots, w_{k+K-1|k}^T)^T$ denoting the disturbance, based on the available information at time instant k.

The disturbances and, hence, the predictions are assumed to be bounded by $\hat{W}_k^{\min} = ((\hat{w}_{k|k}^{\min})^T, \ldots, (\hat{w}_{k+K-1|k}^{\min})^T)^T$ and $\hat{W}_k^{\max} = ((\hat{w}_{k|k}^{\max})^T, \ldots, (\hat{w}_{k+K-1|k}^{\max})^T)^T$, leading to

$$\hat{W}_k^{\min} \leq W_k \leq \hat{W}_k^{\max}, \tag{6}$$

where the relational operator $\leq$ is interpreted element-wise.

Power sharing and power limits: We introduce a virtual slack bus with power distributed among all thermal generators and storage devices. All units of this slack bus change their power in order to balance the variation of load and renewable infeed. This power sharing is controlled in a decentralised manner. As the value of all disturbances w_k is assumed to be known at time k, the variations can be distributed directly to all running thermal generators and storage units without the need to model explicit communication through frequency (which is the case in droop-control). The factors of the power sharing are chosen such that each generator and storage device provides slack power according to its nominal power. The vector $P_{\mathcal{H}} = ((P_{\mathcal{T}}^N)^T, (P_{\mathcal{S}}^N)^T, \mathbf{0}_{r1}^T)^T$ with $P_{\mathcal{T}}^N \in \mathbb{R}_{0+}^t$, $P_{\mathcal{S}}^N \in \mathbb{R}_{0+}^s$ contains these nominal power values. As only running machines can de- or increase their power, we define the vector of predicted shared variations $\mathbf{H}(\delta_{l|k})w_{l|k}$, where $l \in [k, k+K-1] \subseteq \mathbb{N}_0$ is an optimisation time instant of the MPC and

$$\mathbf{H}(\delta_{l|k}) = \frac{-\operatorname{diag}(P_{\mathcal{H}})\,\delta_{l|k}}{P_{\mathcal{H}}^T \delta_{l|k}} \mathbf{1}_{1m} + \operatorname{diag}\left(\mathbf{0}_{(t+s)d}, \mathbf{I}_r\right),$$

where the first part of the equation represents the power sharing of the grid forming units and the second part a change in RES power due to variations $w_{\mathcal{R},l|k}$. The concatenated matrix for power sharing can then be defined by

$$\mathcal{H}_k = \operatorname{diag}\left(\mathbf{H}(\delta_{k|k}), \ldots, \mathbf{H}(\delta_{k+K-1|k})\right).$$

The total predicted power of a unit $P_{\tilde{i}} = (U_k + \mathcal{H}_k W_k)_{\tilde{i}}$, $\tilde{i} \in [1, hK] \subseteq \mathbb{N}$ is given by the sum of the set point $(U_k)_{\tilde{i}}$ and the variation $(\mathcal{H}_k W_k)_{\tilde{i}}$. At any optimisation time instant, the power of every running unit is restricted by lower and upper bounds $P^{\min}, P^{\max} \in \mathbb{R}^{hK \times hK}$,

$$(\Delta_k)_{\tilde{i}} = 1 \Rightarrow \left(P_{\tilde{i}}^{\min} \leq (U_k + \mathcal{H}_k W_k)_{\tilde{i}} \leq P_{\tilde{i}}^{\max}\right). \tag{7a}$$

Recall, that if a unit is disabled its power infeed is zero, i.e.

$$(\Delta_k)_{\tilde{i}} = 0 \Rightarrow (U_k + \mathcal{H}_k W_k)_{\tilde{i}} = 0. \tag{7b}$$

The need for $\mathbf{H}(\delta_{l|k})$ follows from the fact that in islanded operation consumption, generation and storage power always have to match (see (5b)). The matrix $\mathbf{H}(\delta_{l|k})$ captures the relations of changing load and RES and changing power of thermal generators and storage units. For example, assuming the grid in Fig. 2, $P_{\mathcal{H}} = (1, 1, 0)^T$, $\delta_{l|k} = (1, 1, 1)$ leads to

$$\begin{pmatrix} P_{\mathcal{T},l|k} \\ P_{\mathcal{S},l|k} \\ P_{\mathcal{R},l|k} \end{pmatrix} = \begin{pmatrix} u_{\mathcal{T},l|k} \\ u_{\mathcal{S},l|k} \\ u_{\mathcal{R},l|k} \end{pmatrix} + \underbrace{\begin{pmatrix} -\frac{1}{2} & -\frac{1}{2} \\ -\frac{1}{2} & -\frac{1}{2} \\ 0 & 1 \end{pmatrix}}_{\mathbf{H}((1,1,1)^T)} \begin{pmatrix} w_{\mathcal{D},l|k} \\ w_{\mathcal{R},l|k} \end{pmatrix}, \text{ and}$$

$$\begin{pmatrix} P_{\mathcal{T},l|k} \\ P_{\mathcal{S},l|k} \\ P_{\mathcal{R},l|k} \\ w_{\mathcal{D},l|k} \end{pmatrix} = \begin{pmatrix} u_{\mathcal{T},l|k} - \frac{1}{2}(w_{\mathcal{D},l|k} + w_{\mathcal{R},l|k}) \\ u_{\mathcal{S},l|k} - \frac{1}{2}(w_{\mathcal{D},l|k} + w_{\mathcal{R},l|k}) \\ u_{\mathcal{R},l|k} \qquad + w_{\mathcal{R},l|k} \\ w_{\mathcal{D},l|k} \end{pmatrix},$$

i.e. an increase/decrease in the load or RES power leads to decrease/increase of the power from the conventional or the storage unit. This ensures that (5b) is satisfied in the presence of disturbances. If the conventional generation is turned off, i.e. $\delta_{l|k} = (0, 1, 1)$, the disturbances would have to be fully covered by the storage unit and, hence

$$\begin{pmatrix} P_{\mathcal{T},l|k} \\ P_{\mathcal{S},l|k} \\ P_{\mathcal{R},l|k} \\ w_{\mathcal{D},l|k} \end{pmatrix} = \begin{pmatrix} 0 \\ u_{\mathcal{S},l|k} - (w_{\mathcal{D},l|k} + w_{\mathcal{R},l|k}) \\ u_{\mathcal{R},l|k} \qquad + w_{\mathcal{R},l|k} \\ w_{\mathcal{D},l|k} \end{pmatrix}.$$

The dynamics of the storage units are

$$x_{k+1} = \mathbf{A}x_k + \mathbf{B}(u_k + \mathbf{H}(\delta_k)w_k),$$

with $\mathbf{A} = \mathbf{I}_s$, $\mathbf{B} = -t_S\left(\mathbf{0}_{st}, \mathbf{I}_s, \mathbf{0}_{sr}\right)$. Thus, the predicted state for optimisation step $l + 1$, calculated at time instant k is

$$x_{l+1|k} = \mathbf{A}x_{l|k} + \mathbf{B}(u_{l|k} + \mathbf{H}(\delta_{l|k})w_{l|k}),$$

with $x_{k|k} = x_k$, i.e. the initial state of the prediction $x_{k|k}$ is the measured x_k. In the following, the concatenated form

$$X_k = \mathcal{A}x_k + \mathcal{B}U_k + \mathcal{G}_k W_k, \text{ with} \tag{8}$$

$$\mathcal{A} = \begin{pmatrix} \mathbf{I}_s \\ \mathbf{A} \\ \mathbf{A}^2 \\ \vdots \\ \mathbf{A}^{K-1} \end{pmatrix}, \mathcal{B} = \begin{pmatrix} \mathbf{0}_{sh} & \cdots & \cdots & \cdots & \mathbf{0}_{sh} \\ \mathbf{B} & \mathbf{0}_{sh} & \cdots & \cdots & \mathbf{0}_{sh} \\ \mathbf{AB} & \mathbf{B} & \mathbf{0}_{sh} & \cdots & \mathbf{0}_{sh} \\ \vdots & \ddots & \ddots & \ddots & \vdots \\ \mathbf{A}^{K-2}\mathbf{B} & \cdots & \mathbf{AB} & \mathbf{B} & \mathbf{0}_{sh} \end{pmatrix}$$

and $\mathcal{G}_k = \mathcal{B}\mathcal{H}_k$ will be used for convenience. As the storage capacities are limited, the controls must be chosen, such that

$$X^{\min} \leq \mathcal{A}x_k + \mathcal{B}U_k + \mathcal{G}_k W_k \leq X^{\max}, \tag{9}$$

with $X^{\min}, X^{\max} \in \mathbb{R}_{0+}^{sK}$.

The DC power flow between the nodes is given by equations (1)–(5). The predicted generated/consumed power at every node in the network is captured by

$$P_{\mathcal{V},l|k} = ((u_{l|k} + \mathbf{H}(\delta_{l|k})w_{l|k})^T, w_{\mathcal{D},l|k}^T, P_{\mathcal{N}}^T)^T.$$

The passive network nodes with $P_{\mathcal{N}} = \mathbf{0}_{n1}$ were introduced to represent the structure of the grid in an intuitive way and could be reduced, e.g. by Kron reduction [19] in a later step. With the matrices $\mathbf{E}_U \in \mathbb{R}^{vK \times hK}$, $\mathbf{E}_W \in \mathbb{R}^{vK \times mK}$,

$$\mathbf{E}_U = \operatorname{diag}(\mathbf{e}_u, \ldots, \mathbf{e}_u), \mathbf{e}_u = (\mathbf{I}_h, \mathbf{0}_{(d+n)h}^T)^T \text{ and}$$

$$\mathbf{E}_W = \operatorname{diag}(\mathbf{e}_w, \ldots, \mathbf{e}_w), \mathbf{e}_w = (\mathbf{0}_{hm}^T, (\mathbf{I}_d, \mathbf{0}_{dr})^T, \mathbf{0}_{nm}^T)^T$$

we can derive the concatenated vector of all nodal powers

$$\mathcal{P}_{\mathcal{V},k} = \mathbf{E}_U(U_k + \mathcal{H}_k W_k) + \mathbf{E}_W W_k$$
$$= (P_{\mathcal{V},k|k}^T, \ldots, P_{\mathcal{V},k+K-1|k}^T)^T.$$

With $\mathcal{F}'$ and b' from (5), define $\mathbf{F} = \mathrm{diag}(\mathcal{F}', \ldots, \mathcal{F}')$ and $\mathbf{b} = \mathrm{diag}(b', \ldots, b')$. The power flow over the lines is then $\mathcal{P}_{\mathcal{E},k} = \mathbf{F}\mathcal{P}_{\mathcal{V},k}$ and the corresponding constraints read

$$\mathcal{P}_{\mathcal{E}}^{\min} \le \mathbf{F}\mathcal{P}_{\mathcal{V},k} \le \mathcal{P}_{\mathcal{E}}^{\max}, \tag{10a}$$

$$\mathbf{0}_{K1} = \mathbf{b}\mathcal{P}_{\mathcal{V},k}, \tag{10b}$$

where $\mathcal{P}_{\mathcal{E}}^{\min}, \mathcal{P}_{\mathcal{E}}^{\max} \in \mathbb{R}^{eK}$ contain the line power limits.

Short circuit power is taken as a measure for the strength of a grid. It is used instead of the spinning reserve, which is a common indicator for the capability to react to transient events. Droop controlled inverters have a virtual inertia [20] that can be much higher than that of a generator at the same power rating. Consequently, the spinning reserve in microgrids with droop controlled inverters is not connected directly to their behaviour during transient events. Therefore, it is beneficial to use short circuit power, which is limited by the hardware of both inverter and classical generator. The predicted delivered short circuit power of the running machines at time instant l is assumed to sum up to the scalar value $(P_{\mathcal{U}}^{\mathrm{sc}})^T \delta_{l|k}$, where $P_{\mathcal{U}}^{\mathrm{sc}} \in \mathbb{R}_{0+}^h$ is the short circuit power that the units can provide. In every optimisation instant $(P_{\mathcal{U}}^{\mathrm{sc}})^T \delta_{l|k}$ has to be at least as high as the short circuit power that is needed to ensure a safe MG operation $p^{\mathrm{sc}} \in \mathbb{R}_+$. With $\mathcal{P}_{\mathcal{U}}^{\mathrm{sc}} = \mathrm{diag}((P_{\mathcal{U}}^{\mathrm{sc}})^T, \ldots, (P_{\mathcal{U}}^{\mathrm{sc}})^T)$, $\mathcal{P}_{\mathcal{U}}^{\mathrm{sc}} \in \mathbb{R}_{0+}^{K \times hK}$ we can formulate the constraint for all optimisation time instants

$$\mathcal{P}_{\mathcal{U}}^{\mathrm{sc}} \Delta_k \ge p^{\mathrm{sc}} \mathbf{1}_{K1}. \tag{11}$$

D. Optimal Control Problem

Our goal is to minimise a performance index that penalises thermal generation and rewards RES infeed over K time steps. For that, we introduce the weights $C_U \in \mathbb{R}^h$ for power dependent costs, weights $C_{on} \in \mathbb{R}^h$ for power independent costs, and weights to penalise switching a machine on or off $C_{sw} \in \mathbb{R}^h$. A discount factor $\gamma \in (0,1)$ is introduced to emphasise performance in the near future over long-term performance with $\Gamma_U = (\gamma \mathbf{I}_h, \gamma^2 \mathbf{I}_h, \ldots, \gamma^{K-1}\mathbf{I}_h)^T$. The time-weighted vectors for the objective function can be stated as $\mathcal{C}_U = \Gamma_U C_U$, $\mathcal{C}_{on} = \Gamma_U C_{on}$ and $\mathcal{C}_{sw} = \Gamma_U C_{sw}$. Additionally, a switching vector

$$\Delta_{sw,k} = \left| (\delta_{k-1} - \delta_{k|k})^T, \ldots, (\delta_{k+K-2|k} - \delta_{k+K-1|k})^T \right|^T$$

indicates whether machines are predicted to switch from time instant $l-1$ to time instant l for $l = k, \ldots, k+K-1$. Note that the past discrete state δ_{k-1} is used to determine the cost for $l = k$. Thus, the objective function reads

$$J((x_k, \delta_{k-1}), (U_k, \Delta_k)) = \mathcal{C}_U^T U_k + \mathcal{C}_{on}^T \Delta_k + \mathcal{C}_{sw}^T \Delta_{sw,k}.$$

With a worst-case evaluation of the cost, the OCP reads as follows.

Problem 1 (MPC): Find the optimal $(U_k, \Delta_k)^*$ that minimise the cost function

$$\min_{(U_k, \Delta_k)} \max_{W_k} J((x_k, \delta_{k-1}), (U_k, \Delta_k)).$$
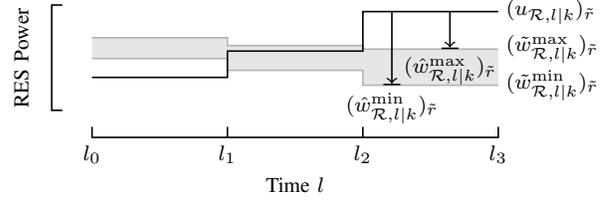
subject to (6)–(11).

Fig. 1. Different cases for RES infeed and disturbance.

III. SOLUTION

In this section, different minimax solutions for Problem 1 will be presented. For that, we will first take a look at the predicted values for the worst-case disturbance.

A. Disturbances

For each time instant l within the optimisation interval at time k, the predicted load lies in the forecast interval, i.e.

$$\hat{w}_{\mathcal{D},l|k}^{\min} \le w_{\mathcal{D},l|k} \le \hat{w}_{\mathcal{D},l|k}^{\max} \tag{12a}$$

where $\hat{w}_{\mathcal{D},l|k}^{\min}, \hat{w}_{\mathcal{D},l|k}^{\max} \in \mathbb{R}^d$, which can be easily incorporated into the optimisation procedure.

In contrast, the predicted fluctuations of the RES depend on the power set point for the corresponding units, i.e.

$$\hat{w}_{\mathcal{R},l|k}^{\min}(u_{\mathcal{R},l|k}) \le w_{\mathcal{R},l|k}(u_{\mathcal{R},l|k}) \le \hat{w}_{\mathcal{R},l|k}^{\max}(u_{\mathcal{R},l|k}). \tag{12b}$$

Recall, that the set points of the RES represent a limitation of the power output. Thus, the predicted worst-case disturbances are only negative, denoting a loss of RES generation. They are calculated for unit $\tilde{r} \in [1, r] \subset \mathbb{N}$ at instant l as follows.

$$(\hat{w}_{\mathcal{R},l|k}^{\min})_{\tilde{r}} = \min((\tilde{w}_{\mathcal{R},l|k}^{\min})_{\tilde{r}} - (u_{\mathcal{R},l|k})_{\tilde{r}}, 0), \text{ and}$$

$$(\hat{w}_{\mathcal{R},l|k}^{\max})_{\tilde{r}} = \min((\tilde{w}_{\mathcal{R},l|k}^{\max})_{\tilde{r}} - (u_{\mathcal{R},l|k})_{\tilde{r}}, 0)$$

where $\tilde{w}_{\mathcal{R},l|k}^{\max}, \tilde{w}_{\mathcal{R},l|k}^{\min} \in \mathbb{R}^r$ are the predicted, weather dependent maximum and minimum possible RES infeeds. There are three possible scenarios for the bounds, depicted in Fig. 1 over three time instants: *i)* From l_0 to l_1, the maximum $(\tilde{w}_{\mathcal{R},l|k}^{\max})_{\tilde{r}}$ and minimum $(\tilde{w}_{\mathcal{R},l|k}^{\min})_{\tilde{r}}$ predicted infeed lie above the limitation $(u_{\mathcal{R},l|k})_{\tilde{r}}$, i.e. unit $\tilde{r}$ is predicted to have a higher guaranteed infeed $(\tilde{w}_{\mathcal{R},l|k}^{\min})_{\tilde{r}}$, than the power that is demanded by the set point. As the RES infeed in this case can be guaranteed, the predicted disturbances $(\hat{w}_{\mathcal{R},l|k}^{\min})_{\tilde{r}}$ and $(\hat{w}_{\mathcal{R},l|k}^{\max})_{\tilde{r}}$ are zero. *ii)* From l_1 to l_2, the set point of $(u_{\mathcal{R},l|k})_{\tilde{r}}$ lies between the bounds of the predicted RES infeed. Thus, the upper perturbation limit $(\hat{w}_{\mathcal{R},l|k}^{\max})_{\tilde{r}}$ can be set to zero as the power cannot exceed the set point $(u_{\mathcal{R},l|k})_{\tilde{r}}$, while the lower disturbance limit is given by the difference between $(\tilde{w}_{\mathcal{R},l|k}^{\min})_{\tilde{r}}$ and $(u_{\mathcal{R},l|k})_{\tilde{r}}$, representing a loss of generation. *iii)* From l_2 to l_3, $(u_{\mathcal{R},l|k})_{\tilde{r}}$ exceeds the predicted lower and upper bound. Hence, the corresponding limits are $(\hat{w}_{\mathcal{R},l|k}^{\min})_{\tilde{r}} = (\tilde{w}_{\mathcal{R},l|k}^{\min})_{\tilde{r}} - (u_{\mathcal{R},l|k})_{\tilde{r}}$ and $(\hat{w}_{\mathcal{R},l|k}^{\max})_{\tilde{r}} = (\tilde{w}_{\mathcal{R},l|k}^{\max})_{\tilde{r}} - (u_{\mathcal{R},l|k})_{\tilde{r}}$, i.e. only negative perturbations are predicted. Then, the predicted minimum and maximum power of unit $\tilde{r}$ equals the predicted non-limited infeed,

$$(P_{\mathcal{R},l|k}^{\min})_{\tilde{r}} = (u_{\mathcal{R},l|k})_{\tilde{r}} + (\hat{w}_{\mathcal{R},l|k}^{\min})_{\tilde{r}} = (\tilde{w}_{\mathcal{R},l|k}^{\min})_{\tilde{r}},$$

$$(P_{\mathcal{R},l|k}^{\max})_{\tilde{r}} = (u_{\mathcal{R},l|k})_{\tilde{r}} + (\hat{w}_{\mathcal{R},l|k}^{\max})_{\tilde{r}} = (\tilde{w}_{\mathcal{R},l|k}^{\max})_{\tilde{r}},$$

This is a common configuration in grids with a small number of installed RES power, where RES infeed is not curtailed.

B. Open-Loop Minimax MPC

With (12), Problem 1 can be restated as follows.

Problem 2 (OLMM MPC): Find the optimal decision variables $(U_k, \Delta_k)^*$ that solve

$$\min_{(U_k, \Delta_k)} \max_{W_k} J\left((x_k, \delta_{k-1}), (U_k, \Delta_k)\right)$$

subject to (6)–(11) and (12).

The presented OLMM approach leads to unnecessarily conservative solutions, as it does not take into account, that in MPC feedback is applied by using the updated, measured state for the next optimisation time instant. This effect can be mitigated by "closing the loop" over the prediction horizon.

C. Closed-Loop Minimax MPC

Traditionally, state feedback control for linear time invariant systems takes the form

$$U_k = \mathcal{L}_{X,k} X_k + V_k, \tag{13}$$

where $V_k \in \mathbb{R}^{hK}$ and $\mathcal{L}_{X,k} \in \mathbb{R}^{hK \times sK}$ are additional real-valued decision variables. Inserting (13) into (8) results in

$$X_k = (\mathbf{I} - \mathcal{B}\mathcal{L}_{X,k})^{-1}(\mathcal{A}x_k + \mathcal{B}V_k + \mathcal{G}_k W_k) \text{ and}$$

$$U_k = \mathcal{L}_{X,k}(\mathbf{I} - \mathcal{B}\mathcal{L}_{X,k})^{-1}(\mathcal{A}x_k + \mathcal{B}V_k + \mathcal{G}_k W_k) + V_k,$$

leads to a nonlinear optimisation problem which is only tractable for small problem setups, i.e. a small number of nodes $\mathcal{V}$ and small optimisation horizon K.

D. Approximate Closed-Loop Minimax MPC

As an alternative to closed-loop minimax MPC, we can use the predicted disturbances to causally parametrise the real-valued controls in a linear manner as proposed by [21],

$$U_k = V_k + \mathcal{L}_k W_k, \text{ with} \tag{14}$$

$$\mathcal{L}_k = \begin{pmatrix} \mathbf{0}_{hm} & \cdots & \cdots & \mathbf{0}_{hm} \\ \mathbf{L}_{10} & \mathbf{0}_{hm} & \cdots & \mathbf{0}_{hm} \\ \vdots & \ddots & \ddots & \vdots \\ \mathbf{L}_{(K-1)0} & \cdots & \mathbf{L}_{(K-1)(K-2)} & \mathbf{0}_{hm} \end{pmatrix},$$

where $V_k = (v_{k|k}^T, \ldots, v_{k+K-1|k}^T)^T$ with $v_{l|k} \in \mathbb{R}^h$, $\mathbf{L}_{10}, \ldots, \mathbf{L}_{(K-1)(K-2)} \in \mathbb{R}^{h \times m}$ and $\mathcal{L}_k \in \mathbb{R}^{hK \times mK}$, respectively. As shown in Section III-A, perturbations from RES depend on the continuous control $u_{\mathcal{R},l|k}$. Therefore, a parametrisation on RES disturbance would still lead to a nonlinear problem, as $\mathcal{L}_k$ is a matrix of free inputs. We can resolve this problem by using only the disturbance of the load for the parametrisation of the inputs, i.e.

$$\mathbf{L}_{ij} = \left(\tilde{\mathbf{L}}_{ij} \quad \mathbf{0}_{hr}\right), \text{ with } \tilde{\mathbf{L}}_{ij} \in \mathbb{R}^{h \times d}.$$

Thus, for $\tilde{i} \in [1, hK] \subset \mathbb{N}$, (7) can be rewritten with (14) as

$$(\Delta_k)_{\tilde{i}} = 1 \Rightarrow \left(P_{\tilde{i}}^{\min} \leq (V_k + (\mathcal{L}_k + \mathcal{H}_k)W_k)_{\tilde{i}} \leq P_{\tilde{i}}^{\max}\right),$$

$$(\Delta_k)_{\tilde{i}} = 0 \Rightarrow ((V_k + (\mathcal{L}_k + \mathcal{H}_k)W_k)_{\tilde{i}} = 0). \tag{15}$$

Similarly, the limits for the predicted state (9) change to

$$X^{\min} \leq \mathcal{A}x_k + \mathcal{B}(V_k + (\mathcal{L}_k + \mathcal{H}_k)W_k) \leq X^{\max}, \tag{16}$$

and the power flow (10) modifies to

$$\mathcal{P}_{\mathcal{E}}^{\min} \leq \mathbf{F}\mathbf{E}_U(V_k + (\mathcal{L}_k + \mathcal{H}_k)W_k) + \mathbf{F}\mathbf{E}_W \hat{W}_k \leq \mathcal{P}_{\mathcal{E}}^{\max},$$

$$\mathbf{0}_{K1} = \mathbf{b}\left(\mathbf{E}_U(V_k + (\mathcal{L}_k + \mathcal{H}_k)W_k) + \mathbf{E}_W W_k\right). \tag{17}$$

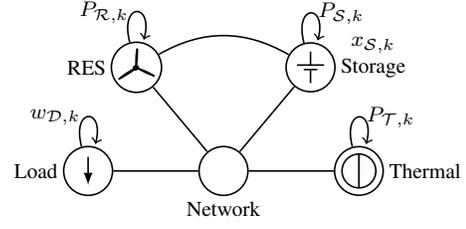Thus, Problem 1 can be restated as follows.

Fig. 2. Microgrid considered for case study.

Problem 3 (ACLMM MPC): Find the optimal decision variables $(V_k, \mathcal{L}_k, \Delta_k)^*$ that solve

$$\min_{(V_k, \mathcal{L}_k, \Delta_k)} \max_{W_k} J((x_k, \delta_{k-1}), (V_k + \mathcal{L}_k W_k, \Delta_k))$$

subject to (11), (12) and (14)–(17).

This problem can be formulated as a mixed-integer linear program (MILP) in a similar way as proposed by [22] and solved numerically online as shown below.

IV. Case Study

In the following numerical case study the operation of a MG in islanded mode with ACLMM MPC will be compared to the operation with mean certainty-equivalence (MCE) and OLMM MPC, both from [11]. Throughout this section all values are normed to a power of 1 pu and a time of 1 h. The microgrid in Fig. 2 is used. It consists of a load $w_{\mathcal{D},k} \in \mathbb{R}$, a RES $P_{\mathcal{R},k} \in \mathbb{R}_{0+}$, a storage device $P_{\mathcal{S},k} \in \mathbb{R}$ and a thermal generator $P_{\mathcal{T},k} \in \mathbb{R}_{0+}$. Hence, $x_k \in \mathbb{R}_{0+}$, $\Delta_k \in \mathbb{B}^3$, $u_k \in \mathbb{R}^3$, $w_k \in \mathbb{R}^2$ and $P_{\mathcal{E},k} \in \mathbb{R}^5$. The limits for the units are $\left(x^{\min}, x^{\max}\right) = (0.167, 0.833)$, $P^{\min} = (0.4, -1, 0)^T$, and $P^{\max} = (1, 1, 2)^T$. Further, the line limits are $P_{\mathcal{E}}^{\max} = -P_{\mathcal{E}}^{\min} = 1.3 \, \mathbf{1}_{51}$, and the parameters for short circuit power $P_{\mathcal{U}}^{\text{sc}} = (1, 1, 0.2)^T$ and $p^{\text{sc}} = 1$. A sampling time of $1/6$ h, i.e. $t_S = 10$ min, resulting in $\mathbf{B} = -(0, 1/6, 0)$ was adopted. The initial conditions $\delta_{-1} = (0, 0, 0)^T$ and $x_0 = 0.2$ were assumed. Further, $C_U = (1, 0, -1)^T$, $C_{on} = 0.1 \cdot \mathbf{1}_{31}$, $C_{SW} = 0.2 \cdot \mathbf{1}_{31}$ and $\gamma = 0.95$ were used. Load and RES profiles according to Fig. 3 were assumed for the simulation. The forecast for the OLMM and ACLMM MPC was given by the bounds $(\tilde{w}_{\mathcal{R},k}^{\min}, \tilde{w}_{\mathcal{R},k}^{\max})$, $(\hat{w}_{\mathcal{D},k}^{\min}, \hat{w}_{\mathcal{D},k}^{\max})$. For MCE MPC, the mean value of the bounds was used as prediction.

An optimisation horizon of $K = 6$ was chosen to incorporate a possible full charge or discharge of the storage unit in the optimisation horizon. The resulting MPC schemes were implemented for a simulation scenario of 5 h. The problem was formulated as a MILP, using Yalmip [23] in MATLAB®, and the solver Gurobi. The computation time at each MPC instant was less than 1 s for the MCE, the OLMM and the ACLMM MPC, with an Intel® Core™ i5-3320M processor @ 2.6 GHz with 8 GB RAM, which is sufficiently fast with respect to the sampling interval of 10 min.

Applying the MCE MPC leads to violations of the power limits at $k = 1$ and $k = 26$ since the uncertainty bounds are not taken into account. The state limits are also violated at $k = 5$, $k = 22$ and $k = 30$. As it can be seen in Fig. 3, the MCE MPC cannot guarantee safe operation. In contrast, using the OLMM and the ACLMM MPC, no limits
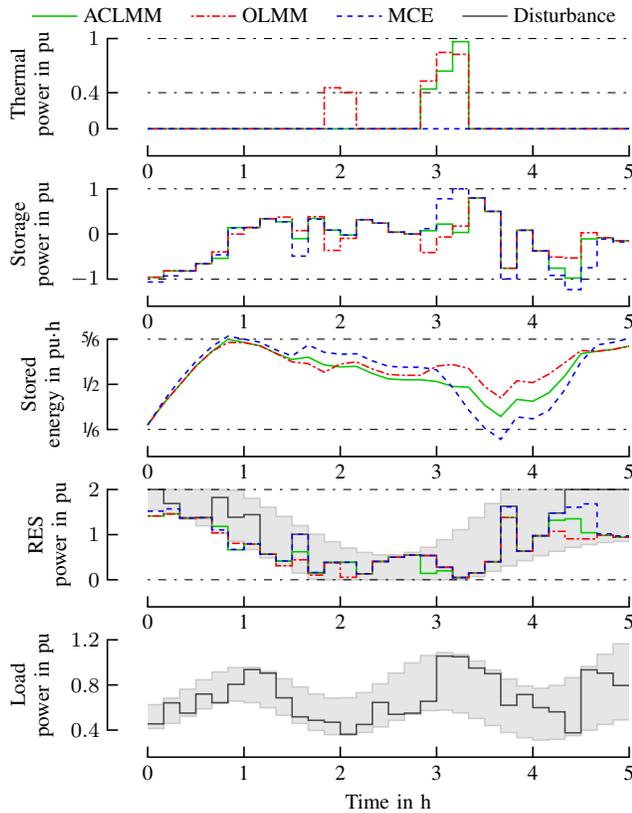
Fig. 3. Thermal, storage, renewable and load power as well as stored energy with different MPC approaches. The grey areas in RES and load power represent the robust interval of the disturbances.

	OLMM	ACLMM
Renewable infeed	20.92	21.93
Thermal infeed	3.06	2.05

are violated, but the RES infeed is lower due to the inherent conservativeness of the approaches. Still, with the ACLMM approach the RES infeed can be increased by 5 % compared to the OLMM MPC. Further, the thermal generator runs longer in the OLMM case than in the ACLMM MPC. Due to the reduced conservativeness of the ACLMM approach, the unit is not turned on at $k = 11$ and $k = 12$. For the considered profiles, this results in a reduction of thermal infeed with the ACLMM MPC of 33 % compared to the OLMM MPC (see Table I). As a direct consequence of the higher RES and lower thermal infeed the ACLMM yields lower costs than the OLMM scheme. However, the cost decrease comes at the price of a higher computational effort, as computing the ACLMM inputs takes twice as long as solving the OLMM problem.

V. CONCLUSIONS

This paper studied the model predictive operation control of microgrids in islanded mode. The problem was solved in an approximate closed-loop minimax manner, where the inputs are parametrised by the disturbance. In the provided numerical case study, the proposed control provides less conservative results than an open-loop approach, leading to an increased infeed of RES and a decrease of thermal generation. Future work will address the optimal operation control of MGs in a probabilistic manner. Further, we plan to apply the approach to a larger case study to assess how the computational complexity scales with the problem size.

REFERENCES

[1] N. Pogaku, M. Prodanovic, and T. C. Green, "Modeling, analysis and testing of autonomous operation of an inverter-based microgrid," *IEEE Trans. on Pow. Electronics*, vol. 22, no. 2, pp. 613–625, 2007.
[2] J. Lopes, C. Moreira, and A. Madureira, "Defining control strategies for microgrids islanded operation," *IEEE Trans. on Pow. Sys.*, vol. 21, no. 2, pp. 916–924, 2006.
[3] M. Arnold, R. Negenborn, G. Andersson, and B. De Schutter, "Multi-area predictive control for combined electricity and natural gas systems," in *2009 ECC*, 2009.
[4] K. Heussen, S. Koch, A. Ulbig, and G. Andersson, "Energy storage in power system operation: The power nodes modeling framework," in *2010 IEEE PES ISGT Europe*, 2010, pp. 1–8.
[5] A. Zafra-Cabeza, A. del Real, A. Arce, E. Camacho, M. Ridao, and C. Bordons, "A risk-based strategy for power system optimization," in *49th IEEE CDC*, 2010, pp. 1905–1910.
[6] A. Parisio, E. Rikos, and L. Glielmo, "A model predictive control approach to microgrid operation optimization," *IEEE Trans. on Control Sys. Technology*, no. 99, 2014.
[7] R. Negenborn, M. Houwing, B. De Schutter, and J. Hellendoorn, "Model predictive control for residential energy resources using a mixed-logical dynamic model," in *IEEE ICNSC*, 2009, pp. 702–707.
[8] D. Bertsimas, E. Litvinov, X. A. Sun, J. Zhao, and T. Zheng, "Adaptive robust optimization for the security constrained unit commitment problem," *IEEE Trans. on Pow. Sys.*, vol. 28, no. 1, pp. 52–63, 2013.
[9] C. Zhao and Y. Guan, "Unified stochastic and robust unit commitment," *IEEE Trans. on Pow. Sys.*, vol. 28, no. 3, pp. 3353–3361, 2013.
[10] R. Jiang, J. Wang, M. Zhang, and Y. Guan, "Two-stage minimax regret robust unit commitment," *IEEE Trans. on Pow. Sys.*, vol. 28, no. 3, pp. 2271–2282, 2013.
[11] C. A. Hans, V. Nenchev, J. Raisch, and C. Reincke-Collon, "Minimax model predictive operation control of microgrids," in *19th IFAC World Congress*, 2014, pp. 10 287–10 292.
[12] J. H. Lee and Z. Yu, "Worst-case formulations of model predictive control for systems with bounded parameters," *Automatica*, vol. 33, no. 5, pp. 763–781, 1997.
[13] P. O. M. Scokaert and D. Mayne, "Min-max feedback model predictive control for constrained linear systems," *IEEE Trans. on Automatic Control*, vol. 43, no. 8, pp. 1136–1142, Aug 1998.
[14] A. Bemporad, "Reducing conservativeness in predictive control of constrained systems with disturbances," in *37th IEEE CDC*, vol. 2, 1998, pp. 1384–1389.
[15] P. Kundur, N. J. Balu, and M. G. Lauby, *Power system stability and control*. McGraw-hill New York, 1994, vol. 7.
[16] K. Purchala, L. Meeus, D. Van Dommelen, and R. Belmans, "Usefulness of dc power flow for active power flow analysis," in *2005 IEEE PES General Meeting*, 2005, pp. 454–459.
[17] J. Schiffer, R. Ortega, A. Astolfi, J. Raisch, and T. Sezi, "Conditions for stability of droop-controlled inverter-based microgrids," *Automatica*, 2014.
[18] J. Schiffer, D. Goldin, J. Raisch, and T. Sezi, "Synchronization of droop-controlled microgrids with distributed rotational and electronic generation," in *52nd IEEE CDC*, 2013, pp. 2334–2339.
[19] F. Dörfler and F. Bullo, "Kron reduction of graphs with applications to electrical networks," *IEEE Trans. on Circuits and Sys. I*, vol. 60, no. 1, pp. 150–163, 2013.
[20] J. M. Guerrero, J. C. Vasquez, J. Matas, L. G. de Vicuña, and M. Castilla, "Hierarchical control of droop-controlled ac and dc microgrids–a general approach toward standardization," *IEEE Trans. on Industrial Electronics*, vol. 58, no. 1, pp. 158–172, 2011.
[21] J. Löfberg, "Approximations of closed-loop minimax mpc," in *42nd IEEE CDC*, vol. 2, 2003, pp. 1438–1442.
[22] A. Bemporad, F. Borrelli, and M. Morari, "Min-max control of constrained uncertain discrete-time linear systems," *IEEE Trans. on Automatic Control*, vol. 48, no. 9, pp. 1600–1606, 2003.
[23] J. Löfberg, "Yalmip: A toolbox for modeling and optimization in matlab," in *2004 IEEE CACSD*, 2004, pp. 284–289.